



Revisiting seasonal dynamics of total nitrogen in reservoirs with a systematic framework for mining data from existing publications

Zhaofeng Guo^{a,b}, Wiebke J. Boeing^c, Yaoyang Xu^{a,d,*}, Changzhou Yan^a, Maede Faghihinia^{a,d}, Dong Liu^{a,b}

^a Key Laboratory of Urban Environment and Health, Fujian Key Laboratory of Watershed Ecology, Institute of Urban Environment, Chinese Academy of Sciences, Xiamen 361021, China

^b University of Chinese Academy of Sciences, Beijing 100049, China

^c Department of Fish, Wildlife & Conservation Ecology, New Mexico State University, Las Cruces, NM 88003, USA

^d Zhejiang Key Laboratory of Urban Environmental Processes and Pollution Control, Ningbo Urban Environment Observation and Research Station, Chinese Academy of Sciences, Ningbo 315830, China

ARTICLE INFO

Keywords:

Reservoir
Total nitrogen
Seasonal dynamics
Data mining

ABSTRACT

Investigation of seasonal variations of water quality parameters is essential for understanding the mechanisms of structural changes in aquatic ecosystems and their pollution control. Despite the ongoing rise in scientific production on spatiotemporal distribution characteristics of water quality parameters, such as total nitrogen (TN) in reservoirs, attempts to use published data and incorporate them into a large-scale comparison and trends analyses are lacking. Here, we propose a framework of Data extraction, Data grouping and Statistical analysis (DDS) and illustrate application of this DDS framework with the example of TN in reservoirs. Among 1722 publications related to TN in reservoirs, 58 TN time-series data from 19 reservoirs met the analysis requirements and were extracted using the DDS framework. We performed statistical analysis on these time-series data using Dynamic Time Warping (DTW) combined with agglomerative hierarchical clustering as well as Generalized Additive Models for Location, Scale, and Shape (GAMLSS). Three patterns of seasonal TN dynamics were identified. In Pattern V-Sum, TN concentrations change in a "V" shape, dropping to its lowest value in summer; in Pattern P-Sum, TN increases in late summer/early fall before decreasing again; and in Pattern P-Spr, TN peaks in spring. Identified patterns were driven by phytoplankton growth and precipitation (Pattern V-Sum), nitrate wet deposition and agricultural runoff (Pattern P-Sum), and anthropogenic discharges (Pattern P-Spr). Application of the DDS framework has identified a key bottleneck in assessing the dynamics of TN — low data accessibility and availability. Providing an easily accessible data sharing platform and increasing the accessibility and availability of raw data for research will facilitate improvements and expand the applicability of the DDS framework. Identification of additional spatiotemporal patterns of water quality parameters can provide new insights for more comprehensive pollution control and management of aquatic ecosystems.

1. Introduction

Reservoirs are artificial freshwater ecosystems built to meet basic water needs for human activities. Purposes of reservoirs include water security to support fundamental human requirements such as drinking water, food, energy as well as human health and general well-being. Although water surface area of reservoirs accounts for only 6% of the global lentic waters, they trap 33% of the total nitrogen (TN) removed from terrestrial ecosystems by lentic systems (nitrogen burial and

denitrification) (Harrison et al., 2009) and serve as important nitrogen storage sites. In reservoir ecosystems, nitrogen plays a key role in sustaining primary production and biogeochemical cycles, and its cellular demand is higher than that of nutrients such as phosphorus and iron (Andersen et al., 2020; Hecky and Kilham, 1988). Nevertheless, negative impacts of excessive nitrogen due to anthropogenic, exogenous, and endogenous loadings (e.g., agricultural fertilization, soil erosion, atmospheric deposition, and decompositions of plants and algae) on reservoir ecosystems and human health (Galloway et al., 2004) have

* Corresponding author at: Key Laboratory of Urban Environment and Health, Fujian Key Laboratory of Watershed Ecology, Institute of Urban Environment, Chinese Academy of Sciences, Xiamen 361021, China.

E-mail address: yyxu@iue.ac.cn (Y. Xu).

<https://doi.org/10.1016/j.watres.2021.117380>

Received 31 March 2021; Received in revised form 17 June 2021; Accepted 18 June 2021

Available online 21 June 2021

0043-1354/© 2021 Elsevier Ltd. All rights reserved.

been well documented. For instance, surplus nutrient loading can lead to non-nitrogen-fixing cyanobacteria becoming superior competitors (Huisman et al., 2018), and resulting cyanobacterial blooms not only deteriorate water quality but also release algal toxins that harm ecological health (Gaget et al., 2017). Water quality problems in reservoirs caused by eutrophication and harmful algal blooms have been of great concern and present a global challenge (Huang et al., 2020). Understanding patterns of seasonal TN dynamics in reservoirs is often a prerequisite for reversing current water quality problems and managing reservoir ecosystems.

Over the past decades, researchers have focused on how to alleviate the above-mentioned negative effects caused by reservoir excess nitrogen and sustainably maintain reservoir ecosystem services. Examples include investigating trophic state and seasonal changes in South Korean reservoirs (Jones et al., 2003), assessing reservoir trophic status and impact on phytoplankton (Xu et al., 2010) and examining spatiotemporal distribution variability of nutrients during a wet and dry year (Williamson et al., 2020). These studies used different data processing and statistical methods to investigate distribution characteristics of water quality parameters at local scales and paradigms cannot be generalized and applied to other reservoirs. To our knowledge, no studies have attempted to analyze reservoir TN dynamics on a global scale and incorporated environmental factors such as climate and hydrology. This is partly due to weak optical activity of reservoir TN, which has spatiotemporal variation and the limited ability to monitor and predict its dynamics by satellite remote sensing (Vakili and Amanollahi, 2020). Fortunately, availability of TN monitoring data for water quality in existing publications offers the potential to meet large-scale trend studies in TN dynamics.

How to mine existing data from the literature and analyze them scientifically and statistically is key to study dynamics of water quality parameters. Most studies that focus on dynamics of environmental parameters over time have collected multi-scale datasets with spatiotemporal variability. Thus, selection of appropriate grouping and fitting methods is beneficial for the interpretation of time-series data and pattern recognition (Li et al., 2021). Time-series clustering methods are powerful tools for analyzing patterns of seasonal dynamics and identifying overall spatiotemporal characteristics of parameters. Among many time-series similarities measures, Dynamic Time Warping (DTW) currently consists of the most widely applied and effective algorithms and is most effective at finding the best alignment and measuring distances (Dupas et al., 2016; Lottig et al., 2017; Wang et al., 2020). Undoubtedly, it is feasible to use DTW to measure distances and differences between time-series data. Furthermore, Generalized Additive Models for Location, Scale and Shape (GAMLSS) was used to fit the seasonal dynamics. This model is widely employed in hydrological time-series modeling as a flexible statistical modeling approach (Li and Tan, 2015; López and Francés, 2013; Su and Chen, 2019).

Here, we proposed a framework of Data extraction, Data grouping and Statistical analysis (DDS framework) aimed at assessing dynamic variations of water quality parameters. Taking TN in reservoirs as an example, the framework is applied to extract and statistically analyze literature data to explore the following research questions: (1) How can time-series data be most efficiently collected from the existing literature? (2) What are the patterns of TN seasonal dynamics in reservoirs? (3) What are the causes of TN dynamics? Application of the DDS framework for TN dynamic exploration contributes to the eutrophication control and management of reservoir ecosystems. Meanwhile, key issues in the data mining and dynamic exploration of water quality parameters with TN as an example were demonstrated, and the significance of current data sharing and improving the accessibility and availability of raw data to promote pollution management in aquatic ecosystems is emphasized.

2. Methods

The DDS framework shown in Fig. 1 demonstrates whole process of extracting, grouping and statistically analyzing the time-series data, taking reservoir TN as an example. First, retrieved literatures are screened and time-series data are extracted. Then, obtained time-series data are sorted and grouped. Finally, time-series clustering and fitting are performed on the data sets that met analytical requirements to obtain TN patterns. Combined with other environmental factors, the causes of seasonal variations of TN were identified.

2.1. Data extraction

First, a search was performed in Web of Science Core Collection for literature published from 1990 to 2020 using the terms “reservoir” AND “nutrient” AND “nitrogen” in the Web of Science “Topic” search (Fig. 1a). The scope of “Topic” search includes the title, abstract, and keywords list of the publication. A total of 1722 documents were retrieved. Among the retrieved documents, 1351 were available for download as PDF files. Then, we reviewed the full texts of these 1351 documents and found 909 that contained surface water data from the reservoirs. Further manual screening identified 113 documents containing TN dynamics data, and the remaining documents that did not provide TN data or only measured other forms of nitrogen data were excluded. These data were presented in 21 tables and 97 figures within the 113 documents. We obtained those data either directly from tables or using the GetData Graph Digitizer software (V2.26; <http://www.getdata-graph-digitizer.com/>) from figures. Some studies performed multi-point or stratified sampling, i.e., multiple time series could be obtained in these studies. Thus, a total of 172 time-series were obtained.

2.2. Data grouping

The 172 extracted time-series data were classified into ‘annual’, ‘seasonal’, ‘monthly’, ‘weekly’, and ‘daily’ sampling frequencies (Fig. 1b). Analyses of TN concentrations on a quarterly or annual monitoring frequency mask seasonal dynamics of reservoir ecosystem structure and other environmental factors (Kong et al., 2019), and these data were not considered. Daily- and weekly-scale data were excluded from this study due to absence of 12-period monitoring or missing data or the fact that data were averaged. Moreover, ‘monthly’ time scale accounted for more than 68% (117) of TN time-series, and thus, we focused our analyses on those data.

TN data were then classified as to whether they were based on averaged or non-averaged data. We discarded the 35 time-series that only provided averaged monthly data. The remaining 82 data that provided non-averaged data were subdivided into three categories based on the duration of their monitoring. Time-series with a monitoring duration shorter than 12 months (24 time-series) were excluded from this study as they did not provide a complete annual picture of TN dynamics. To facilitate analyses of monthly time-series of different durations, this study cut data series that had monitoring data between 12 and 24 months (37 time-series) to a consistent 12-month time span. Time-series that exceeded 24 months were split into 21 sub-series with 12 months duration each. The 58 time-series were further classified according to their spatial data collecting protocol: single-point, multipoint, layered, and multipoint layered (sampling of various water depths) sampling.

Overall, we analyzed 58 time-series from 19 different reservoirs (Table S1). We retrieved a single time-series from eleven reservoirs. For eight reservoirs we were able to extract between 2 to 12 time-series data. Data sets that stemmed from the same reservoir were either collected at different times, locations, or water depths. Processing of the above time series is based on our assumption that TN dynamics from the same reservoir may also vary depending on sampling time, location, and water depths (See Section 3.2 for a detailed discussion). Usage of

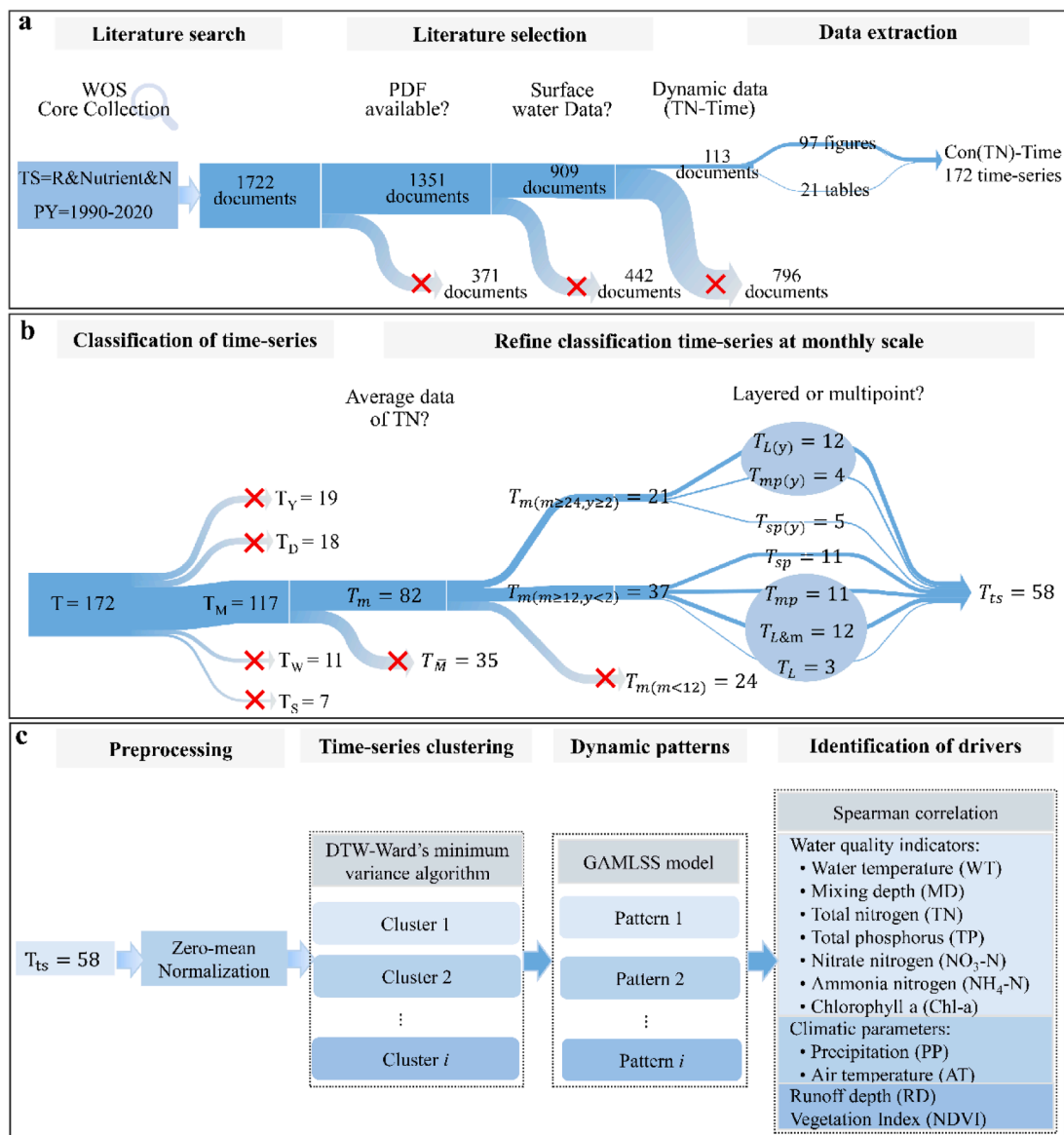


Fig. 1. Data extraction, Data grouping and Statistical analysis framework (DDS framework). The red "X" mark indicates that the data was excluded. (a) Data extraction; WOS – Web of Science; TS – Topic Search; R – Reservoir; N – Nitrogen; PY – Publication Year; (b) Data grouping. Sampling frequency: annual (T_Y), seasonal (T_S), monthly (T_M), weekly (T_W), and daily (T_D). Spatial sampling distribution: single-point (T_{sp}), multipoint (T_{mp}), layered (T_L), layered and multipoint ($T_{L\&m}$); (c) Statistical analysis. (For interpretation of the references to color in this figure legend, the reader is referred to the web version of this article.)

averaged data could have made the true trends of TN patterns invisible during our analyses.

2.3. Statistical analysis

The time-series data were standardized to a mean of 0 and a standard deviation of 1 before analyses (Fig. 1c). An agglomerative hierarchical cluster was performed to group TN time-series using Ward's minimum variance algorithm with Dynamic Time Warping (DTW). DTW algorithm was used to measure distances between clusters with the smallest sum of squared deviations and is calculated based on the minimum distance of all possible alignments (Sakoe and Chiba, 1978). We used the "dtw" package in the R software for time-series cluster analysis.

Once clusters were identified, Generalized Additive Model for Location, Scale and Shape (GAMLSS) with cubic spline regression was applied to fit patterns of TN seasonal dynamics of all time-series in each cluster. As a semiparametric or parametric regression model, GAMLSS relaxes the assumptions about the type of distribution of the response

variables and can describe any linear or non-linear relationship between the variables (Rigby and Stasinopoulos, 2005). Best-fitting distribution was selected based on values of the Akaike Information Criterion (AIC) during GAMLSS fitting. The "gamlss" package in the R software was used to run GAMLSS models.

To investigate the causes of TN dynamics, we also collected data on basic information, water quality indicators, climatic parameters, runoff depth, and Normalized Difference Vegetation Index (NDVI) from the literature and related data-sharing platforms (Table S1; Parameter data). Among them, the following data were collected from the literature containing TN dynamic data: sampling dates, latitude and longitude of sampling sites, monthly concentrations data of total phosphorus, nitrate-N, ammonia-N, and chlorophyll-a (Chl-a). The extraction and pre-processing method of water quality parameters data are consistent with that of TN time series data. Not all literature contains the above data, but at least sampling dates information is required. Precipitation, air temperature, mixing depth, water temperature, and runoff depth were obtained from the Climate Data Store. NDVI data were downloaded

from the NASA Earth Observation website. To reduce the uncertainty of analysis, data obtained from the database were selected for periods corresponding to the TN sampling dates. The specific sources and information of each parameter were detailed in Table S1 (Parameter information). Spearman correlation analyses were performed on monthly datasets of climatic parameters, water quality indicators, runoff depths, and NDVI. We used the "openair" package in the R software to run correlation analysis.

3. Results

3.1. Geographical coverage of total nitrogen (TN) time-series dataset

The 58 monthly TN time-series data used for analyses originated from 19 reservoirs on five continents (Fig. 2), with broad geographical coverage but were located mainly in Asia (10 reservoirs) and Europe (5 reservoirs). The remaining time-series were extracted from Belle Mina Reservoir and Lake Waco Reservoir (USA), Pao-Cachinche Reservoir (Venezuela) and Yaacoub Al Mansour Reservoir (Morocco). Detailed information on the location of the reservoirs can be found in Supplementary Materials (Table S1; Reservoir information).

3.2. Spatiotemporal characterization of TN dynamics

TN time-series data were divided into three clusters (Fig. 3). Twenty-two TN time-series from nine reservoirs on five continents formed Cluster 1. TN concentrations in this cluster ranged from 0.03 to 9.12 mg L⁻¹, with an average of 1.44 ± 1.31 mg L⁻¹. The coefficient of variation reached 90.62% and the degree of data dispersion was high. The average, upper and lower quartiles, and the peak of probability density function distribution for Cluster 1 were all lower than for Cluster 2 and 3. The 16 TN time-series in Cluster 2 were from eight reservoirs on four continents, with TN ranging from 0.37 to 5.42 mg L⁻¹ and an average of 1.92 ± 1.01 mg L⁻¹. The coefficient of variation was 52.61% and the degree of data dispersion was relatively small. For Cluster 3, the 20 TN time-series came from nine reservoirs on four continents. TN concentrations in this cluster ranged from 0.20 to 13.76 mg L⁻¹ with an average

of 2.59 ± 2.16 mg L⁻¹ and a coefficient of variation of 83.33%. In contrast, the average and upper quartile values for Cluster 3 were higher than those for Cluster 2.

TN time-series from multiple sampling sites within an individual reservoir were not all spatially similar in their TN dynamics, and TN sub-time-series from same sampling sites over multiple years were not all temporally similar. For example, while the six time-series data collected from different sampling locations of Three Gorge Reservoir all fell into Cluster 2, the data from five different sampling locations from Qingcaosha Reservoir were separated into Clusters 1 and 2. And the four time-series data stemming from different water surface sampling sites of Pao-Cachinche Reservoir ended up in Clusters 2 and 3. Similarly, data sets from different water layers / depths could cluster together (Pao-Cachinche Reservoir) or separate (Shingu Reservoir, Simajigawa Reservoir) and data sets retrieved from the same reservoir but during different years could end up in the same (Baihua Reservoir; Lake Glebokie Reservoir; Simajihawa Reservoir, surface layer) or different clusters (Belle Mina Reservoir; Simajihawa Reservoir, middle and bottom layers).

Three patterns of seasonal TN dynamics were identified by fitting the time-series in each cluster using the cubic spline function of the GAMLSS model. Pattern 'Summer Valley' (V-Sum) fit a Power Exponential, Pattern 'Summer Peak' (P-Sum) an ex-Gaussian, and Pattern 'Spring Peak' (P-Spr) a Skew Normal Type 2 distribution. Filliben correlation coefficients were greater than 0.98 for all models and the quality of fit met analytical requirements in all cases. The lowest TN concentration for Pattern V-Sum is reached during the summer resulting in a "V" shape (Fig. 4a). In Pattern P-Sum, TN concentration increased in spring, peaked in summer, and then decreased again reaching its lowest values during the winter months (Fig. 4b). In Pattern P-Spr, TN increased early in the year and reached a peak in spring and decreased during the summer and fall (Fig. 4c).

3.3. Correlation between TN and other environmental factors

To investigate the causes of TN seasonal dynamics, Spearman correlations between climate parameters, water quality indicators, monthly

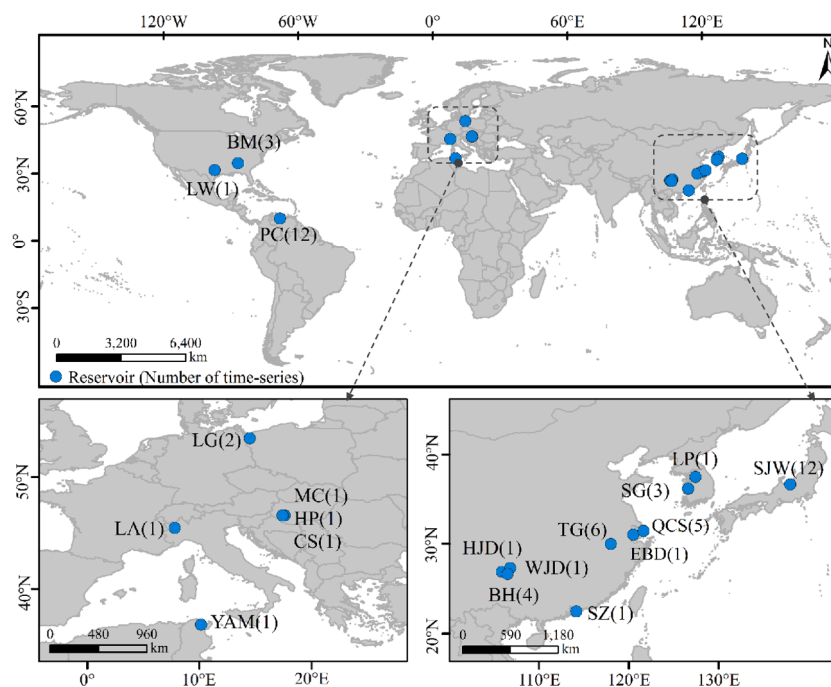


Fig. 2. The geographic location of the 19 reservoirs where total nitrogen (TN) was monitored for more than 12 months: 3 in Americas; 6 in Europe/North Africa; and 10 in Asia. The value after the reservoir name is the number of time-series.

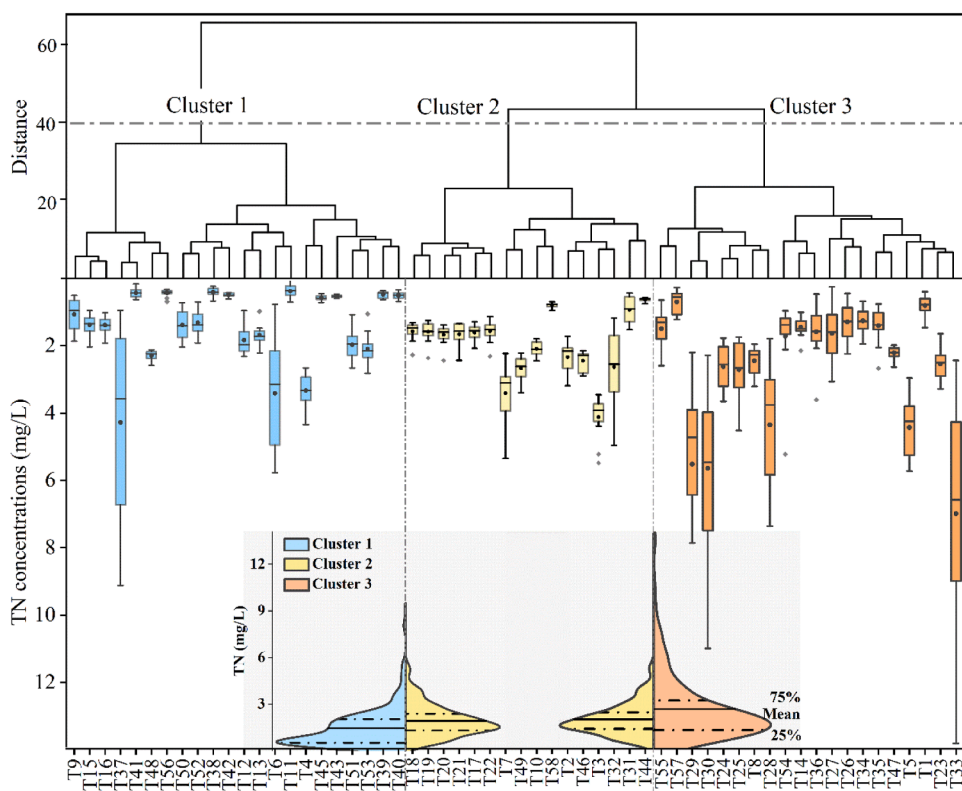


Fig. 3. Total nitrogen (TN) time-series clustering and its distribution of concentration characteristics for each cluster. Cluster analysis diagrams were obtained with Dynamic Time Warping (DTW) Agglomerative Hierarchical Clustering Algorithm (top). Boxplots are based on monthly TN time-series (bottom); boxes represent interquartile ranges of 25 and 75%, horizontal lines in boxes show medians, black dots are means, and whiskers represent 1.5 times the interquartile range (IQR). The x-axis shows the data and corresponds to “Sample Code” in Table S1. Split violin plots show the distribution of TN concentration for each cluster; dashed lines correspond to the lower and upper quartiles and black solid line lines represent the mean; the outer shape is the kernel density estimate (the density of data distribution).

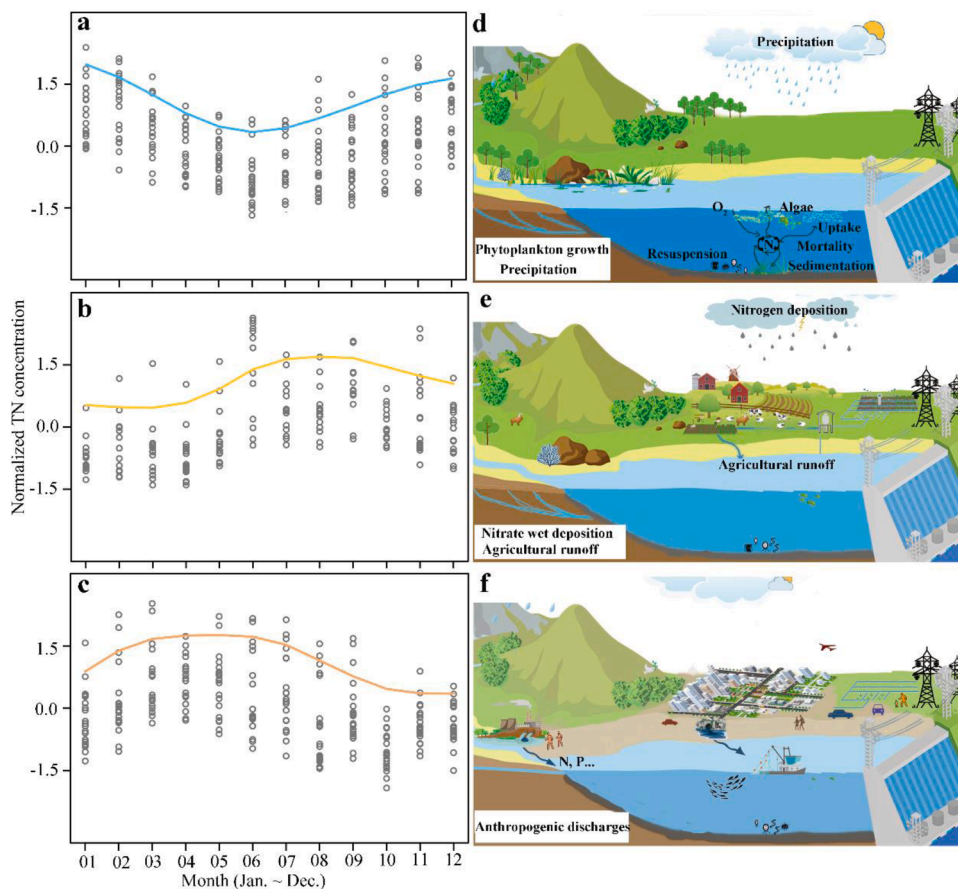


Fig. 4. Centiles plots of the total nitrogen (TN) monthly dynamics based on Generalized Additive Models for Location, Scale, and Shape (GAMLSS) (a, b, and c) and their corresponding pattern diagrams (d, e and f). The line is the regression estimation curve for the 90%quantile($p < 0.01$).

runoff depths, and Normalized Difference Vegetation Index (NDVI) were analyzed. In Pattern V-Sum, there were significant and strong positive correlations between TN and TP as well as TN and nitrate-N ($r = 0.59$ and 0.75 , respectively, $p < 0.01$) and negative correlations between TN and precipitation, TN and NDVI, as well as TN and mixing depth ($r = -0.21$, -0.27 , and -0.43 , respectively, $p < 0.01$) (Fig. 5a). In Pattern P-Sum, there were weak positive correlations between TN and TP ($r = 0.25$), TN and monthly runoff depth ($r = 0.21$), and a negative correlation between TN and mixing depth ($r = -0.45$) (Fig. 5b). In Pattern P-Spr, TN was correlated with nitrate-N ($r = 0.78$), TP ($r = 0.64$), and Chl-a

($r = 0.52$) ($p < 0.01$ in all cases) (Fig. 5c). Like the two previous patterns, mixing depth was again negatively correlated with TN ($r = -0.88$) in Pattern P-Spr. Additionally, all three patterns showed strong negative correlations between TP and TN/TP mass ratio ($r = -0.74$, $r = -0.88$, and $r = -0.78$, respectively; $p < 0.01$ in all cases). In all three patterns, the three parameters, TN and air temperature as well as water temperature, clustered in the same cluster but did not show significant correlations.

4. Discussions

4.1. Pattern V-Sum and its potential causes

Phytoplankton communities play an important role in TN dynamics in Pattern V-Sum (Fig. 4d). The negative correlation between TN and NDVI further confirmed that phytoplankton growth likely influenced TN concentration. During the growth period, phytoplankton take up more nutrients thus reducing their concentration and resulting in the lowest TN concentrations during the summer (Yang et al., 2020). Nitrate-N concentrations showed similar trends to TN (Fig. S1b) and were negatively correlated with water temperature. This could be the result of increased water temperature, reduced reservoir load and enhanced phytoplankton uptake and denitrification during summer months (Wang, 2020). Phytoplankton accelerates the deposition of nutrients and prevents their resuspension of nutrients from the sediment, contributing to stabilization of the water column and further reducing nutrient concentrations (Qi et al., 2019). The low-temperature winter conditions in the reservoir inhibit aquatic biological activity and lead to low oxygen consumption, which decreases the absorption, adsorption, and deposition of nutrients. As a result, TN content was higher in both fall and winter compared to summer.

TN dynamics of Pattern V-Sum were also related to monthly precipitation. Precipitation patterns are the potential factor in changing the dynamics of water quality parameters (Atique and An, 2020). The negative correlation between TN and monthly precipitation indicates that precipitation affected seasonal variations in TN. Summer-dominated precipitation (especially in June) caused a significant decrease in TN concentrations due to dilution effects (Fig. S1i). Furthermore, large amounts of runoff that converge after heavy precipitation promote reservoir mixing, increase dissolved oxygen levels in the water-body and inhibit release of nutrients from the sediment, resulting in lower algal biomass in the reservoir (Li et al., 2015). Chl-a concentrations and Chl-a/TN ratios showed a decreasing trend in summer, and we speculate that dilution effect of TN and algae caused by heavy precipitation was stronger during this period. TP dynamics in spring and summer were synchronous with TN and there was a moderate negative correlation between TP and precipitation. This is consistent with the hypothesis that precipitations have a diluting impact on nutrients (Dupas et al., 2018).

TN/TP, Chl-a/TN, and Chl-a/TP ratios are often used as indicators of potential nutrient limitation in reservoirs (Spears et al., 2013). Compared to the other two patterns, Chl-a/TP ratios were relatively high in Pattern V-Sum and more than 60% of TN/TP ratios were greater than 22.6, indicating phosphorus acts as a potentially limiting factor (Mamun et al., 2020; Qin et al., 2020). Chl-a/TN ratios increased and then decreased in the first half of the year, probably due to dilution of TN resulting in transient nitrogen limitation of algae. The time-series samples in Pattern V-Sum were mainly from drinking water reservoirs, such as Qingcaosha Reservoir and Shimajigawa Reservoir, where the nutrient loads mainly stemmed from natural origin (Chen and Zhu, 2018; Komatsu et al., 2006). In short, TN dynamics in Pattern V-Sum were primarily influenced by phytoplankton activity and precipitation and were subject to relatively little human perturbation and had a more healthy / natural catchment area.

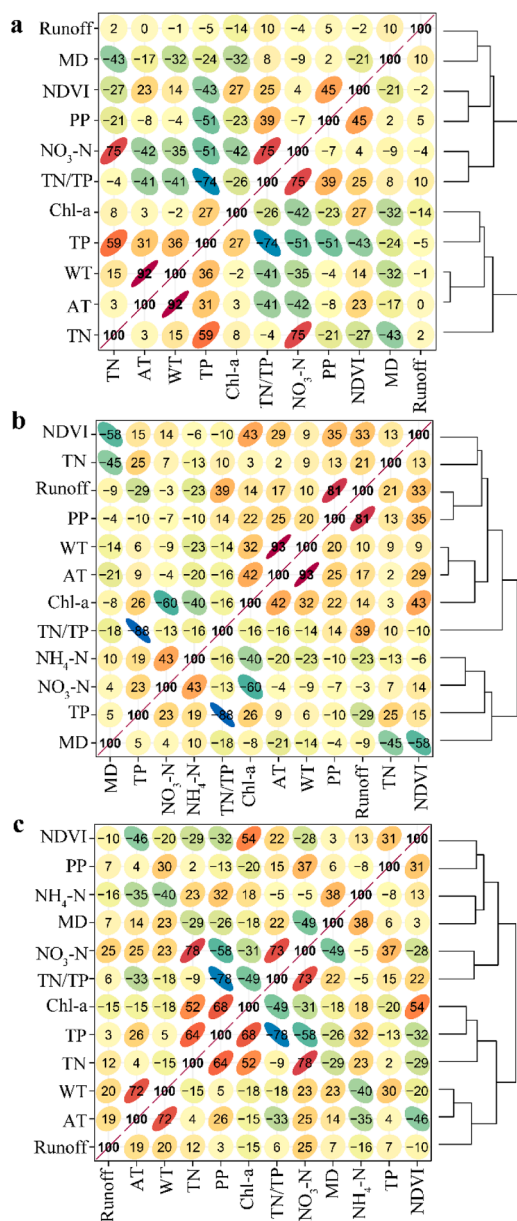


Fig. 5. Correlation matrix heatmap. Correlations between parameters are shown by shape/tilt, and value. An oval shape with a tilt represents the positive or negative correlation. Correlation coefficients of -1 and 1 correspond to a tilt of 135° and 45°, respectively. $R = 0$ corresponds to a circle. The value (number inside the shape) shows the percentage of the correlation coefficient (r^*100). Hierarchical clustering is applied to the correlation matrices to group similar parameters (right of figure). AT – air temperature; Chl-a – chlorophyll-a; MD – mixing depth; NDVI – Normalized Difference Vegetation Index; $\text{NH}_4\text{-N}$ – ammonia-nitrogen; $\text{NO}_3\text{-N}$ – nitrate-nitrogen; PP – total precipitation; RD – monthly runoff depth (the sum of surface runoff and sub-surface runoff); TN – total nitrogen; TP – total phosphorus; WT – water temperature.

4.2. Pattern P-Sum and its potential causes

Nitrate wet deposition and agricultural runoff were the factors that dominated TN dynamics in Pattern P-Sum (Fig. 4e). A comparison of nitrate-N concentrations with corresponding precipitation distribution showed a relationship between nitrate-N and precipitation peaking at the same time in summer (June) (Fig. S1b and i). Nitrate wet deposition may be the cause of increased nitrogen load in summer because atmospheric nitrogen may have been transformed to nitrate-N by nitrification and reached reservoir areas in the form of precipitation (Hao et al., 2017). However, TN was not strongly correlated with nitrate and ammonia-N and its concentration did not increase to its peak until late summer. This may have been caused by surface runoff accumulating after the precipitation period and carrying large amounts of nutrient-rich pollutants into the water (Wang et al., 2018). This hypothesis is supported by the positive correlation between TN and monthly runoff depth (the sum of surface runoff and sub-surface runoff).

Precipitation-induced soil erosion can cause an increase in TP and TN loads of water (Leigh et al., 2010). But while TP and runoff depth were negatively correlated, neither one exhibited a strong correlation with TN. This indicates that TN was not primarily derived from soil erosion. Additionally, nitrate-N is closely related to leaching of agricultural nitrogen fertilizers (Ferrier et al., 2001). Following heavy precipitation events in summer, nitrate-N concentrations in Pattern P-Sum were higher than those in the other two patterns and the high proportion of nitrate-N compared to ammonia-N. This probably demonstrates that agricultural runoff has a greater influence on TN dynamics compared to urban inputs (Al-Taani, 2011). Chl-a and TN reached the highest values during the same season, indicating that stored nutrients and warmer temperatures tend to trigger algal blooms in the summer. A decreasing trend in TN concentrations began in the fall, which was associated with a decrease in agricultural runoff.

4.3. Pattern P-Spr and its potential causes

TN dynamics in Pattern P-Spr were mainly attributed to anthropogenic discharges (Fig. 4f). A majority of time-series samples for this pattern were taken from Pao-Cachinche Reservoir and Glebokie Lake, which receive untreated wastewaters from human and animal, resulting in eutrophic-hypertrophic state (Gonzalez et al., 2004; Miller et al., 2016). TN/TP ratios of Pattern P-Spr were relatively low compared to the other patterns (Fig. S1g). Reservoirs that are more subjected to agricultural and urban runoff tended to have lower TN/TP ratios compared to reservoirs that are exposed to fewer human disturbances (Mamun et al., 2020). In the TN composition, the average proportion of inorganic nitrogen reached more than 57% and the proportion of nitrate-N and ammonia-N was equal, which may be attributed to sewage discharge (Grabb et al., 2021; Vilmin et al., 2018b). Positive correlations between TN and nitrate-N ($r = 0.78$) as well as TN and ammonia-N ($r = 0.23$) further indicated that anthropogenic activities, such as agricultural, industrial, and domestic sewage, were the main sources of nitrogen contamination (Guo et al., 2020).

Agricultural wastewater discharges are most likely to contribute to TN dynamics in Pattern P-Spr. Activities such as tillage and irrigation are particularly frequent in spring. This is accompanied by the discharge of agricultural wastewater rich in nutrients, resulting in abnormally high levels of TN during this period (Zhang et al., 2020). As crops are harvested and agricultural activities decrease, TN concentrations decrease. Most of the time-series samples in this pattern were located at shallower depth locations, such as those at Globokie Lake and Marcali Reservoir, where the water depth was less than 2.5 m (Matyas et al., 2003; Miller et al., 2016). Thus, external anthropogenic disturbances had a greater impact on their water chemistry. Pattern P-Spr exhibited higher levels of Chl-a and TN concentrations compared to the other two patterns (Fig. S1f). This is attributed to the fact that reservoirs located in agricultural and urban areas receive relatively more nutrients (Atique and

An, 2020). In Pattern P-Spr, the increased spring temperature in spring has potential to stimulate phytoplankton growth, i.e., excessive nutrient accumulation is likely to trigger algal blooms in spring (Liang et al., 2020). Chl-a increased substantially in spring, probably because excess nutrient storage tended to trigger algal blooms during that time. Most of the TN, especially in Patterns P-Sum and P-Spr were greater than 1 mg L^{-1} , demonstrating that most reservoirs are nitrogen-rich waters. The correlation between Chl-a and TP was stronger compared to Chl-a and TN. This suggests that TP had more influence on changes of aquatic biomass in nitrogen-rich waters, which is consistent with the results of other lakes and reservoirs studies (Søndergaard et al., 2017; Wang, 2020).

4.4. Challenge of pattern analysis and significance of data availability and sharing

We identified TN dynamics in reservoirs, but due to limited data, there may still be other patterns that were not detected. In this study, we did not use the TN data from two ice-covered reservoirs. On one hand, because of a small amount of data and inconsistency of the ice-cover period between reservoirs (He et al., 2011; Shourian et al., 2016), comparative analyses could not be carried out and general conclusion could not be drawn. On the other hand, full ice cover has an impact on both the structure and function of aquatic ecosystem (McMeans et al., 2020), and reservoir TN dynamics may show another completely novel pattern. With the growing number of publication data, the DDS framework can be further improved and applied to separate studies of TN dynamics for ice-covered reservoirs in future work. By further improving the DDS framework, a separate discussion of TN dynamics for ice-covered reservoirs should be conducted in future.

Results of data extraction and grouping from reservoirs demonstrated the low accessibility and availability of raw data for a large number of studies. In some of the literature where data were accessible, sampling details including geographic location, number of sampling sites and distance from the dam were not indicated in the text, reducing data availability. In response to this shortcoming, scholars in the field of hydrology have developed survey tools for self-assessment of data availability and reproducibility to aid authors in evaluating their manuscripts and improve data accessibility before publication (Stagge et al., 2019), which are worth replicating in other fields.

Inappropriate processing of raw data reduces results credibility and data availability. TN variability in reservoirs is subject to a combination of regional hydrologic disturbances and internal regulatory mechanisms, and even TN dynamics in the same reservoir often exhibit asynchronous patterns across sampling location, depths, and interannual. For example, the Pao-Cachinche Reservoir (Venezuela), mentioned above, is used for drinking water supply and agricultural irrigation but can have untreated municipal and farming wastewater sinks in its watershed (Gonzalez et al., 2004). This large reservoir has different seasonal dynamics of nitrogen patterns at different sampling sites. Within a reservoir ecosystem, its physical, chemical, and biological factors interact and exhibit multi-dimensional variability (Xu et al., 2012), thus driving spatiotemporal heterogeneity of water quality parameters. This also means that the average value of multiple/stratified sampling points or multi-year may not necessarily represent trends of nutrient dynamics. Nearly 30% of monthly TN time-series were averaged without considering spatiotemporal differences, smoothing and masking out variability on spatiotemporal scales. Thus, we decided not to utilize those data which was also a cause of the low data availability of TN time-series. This also demonstrates the necessity to understand how various parameters fluctuate synchronously or asynchronously on a spatiotemporal scale before determining monitoring protocols and data processing methods for long-term observations of aquatic ecosystem dynamics (Vilmin et al., 2018a).

Data sharing and extensive data accumulation at spatiotemporal scales are key to future explorations of patterns of seasonal dynamics of

environmental parameters in reservoir ecosystems on a global scale. Some popular study areas (e.g., Three Gorges Reservoir) were monitored by different institutions over the same time period. However, due to the lack of collaborations, cooperation, and sharing mechanisms, monitoring data and results were not well integrated and explored. Improvements in data sharing would allow us to assess potential water quality problems from a global perspective. At the regional level, many studies have been conducted on TN in reservoirs, with the highest foci in North America, Europe, and Asia. This reflects the capacity for large-scale studies in these regions and offers the possibility to create global datasets with broad geographic coverage. However, TN time-series extracted from South America and Africa are still limited. Indeed, our ability to accurately assess the dynamics of global reservoir TN relies on the accumulation of a range of spatiotemporal scale observations. Integrating spatiotemporal data into a framework and applying them in analyses of seasonal dynamics in reservoir ecosystems will provide new insights into the mechanisms that dynamics of environmental parameters in reservoirs in general.

5. Conclusion and future suggestions

In this study, a data extraction, data grouping and statistical analysis framework (DDS framework) was proposed for identifying seasonal dynamics of water quality parameters. Workflow of DDS framework was illustrated with the example of total nitrogen (TN) in reservoirs. With a total of 1722 publications, our employment of this framework produced 58 time-series data of TN from 19 reservoirs, indicating that accessibility and availability of monthly data for TN provided in the publications were not high. Among the three patterns of TN seasonal dynamics identified, TN concentrations in Pattern V-Sum showed a decreasing and then increasing trend over the year with a minimum value occurring in early summer. Phytoplankton growth and precipitation were the main causes of this pattern. In Pattern P-Sum, TN was mainly influenced by nitrate wet deposition and agricultural runoff, which tends to first increase during the year and then decrease, reaching a peak in later summer. In Pattern P-Spr, the peak in TN concentrations occurred in spring, with a decreasing trend after early summer and was mainly caused by anthropogenic discharges. Understanding the TN seasonal dynamics in reservoirs will help in reservoir water quality pollution control and management.

The underlying mechanisms of TN patterns and their causes are still at a high level of uncertainty. Low data accessibility and availability constrain further exploration of TN dynamics in reservoirs. Dynamics of water quality parameters in reservoir ecosystems are often influenced by complex biotic and abiotic interactions. This means that most patterns of seasonal dynamics cannot be characterized by linear models. TN dynamics may be influenced by multiple and uncertain sources, especially in large reservoirs, where the diversity of pollution sources allows for spatiotemporal heterogeneity in nitrogen dynamics. However, data gaps in some water quality parameters limit the interpretation of TN dynamics. For example, Chl-a and air temperature, as indicators affecting ecological status of water quality as well water temperature and runoff in reservoir ecosystems respectively, did not show the expected correlations with TN in Patterns V-Sum and P-Sum. This indicates that TN has a complex relationship with these parameters and is also controlled by other environmental factors not considered.

Application of this DDS framework identifies primary issues to be addressed in spatiotemporal dynamic studies of water quality parameters, i.e., emphasizing the significance of data sharing and the necessity to improve accessibility and availability of raw data. Sharing raw data through easily accessible platforms can increase the efficiency of reusing published data and facilitate deeper information mining. Because of spatiotemporal heterogeneity of dynamic variations in water quality parameters, data processing without considering characteristics of parameter variations will also affect the availability of accessible data. Therefore, data sharing needs to take into account principles of

accessibility and reusability. The proposed DDS framework can be extended to other aquatic ecosystems to identify more parameter dynamics while providing guidance for more comprehensive ecosystem pollution control and management.

Declaration of Competing Interest

We declare that we do not have any commercial or associative interest that represents a conflict of interest in connection with the work submitted.

Acknowledgments

This research was supported financially by Ministry of Science and Technology of China (MSTC) with National Key Research and Development Program (2017YFE0119000) and National Natural Science Foundation of China (NSFC) with Young Scientists Programs (No. 31200358; 31300397). Special thanks to Zhongyao Liang for providing guidance on the clustering method in this study. Authors are grateful to the editor and the two anonymous reviewers for their constructive comments and suggestions to improve this manuscript. Any opinions, findings, and conclusions or recommendations expressed in this work are those of the authors and do not necessarily reflect the views of MSTC and NSFC.

Supplementary materials

Supplementary material associated with this article can be found, in the online version, at doi:[10.1016/j.watres.2021.117380](https://doi.org/10.1016/j.watres.2021.117380).

References

- Al-Taani, A.A., 2011. Seasonal variations in water quality of Al-Wehda Dam north of Jordan and water suitability for irrigation in summer. *Arab. J. Geosci.* 6 (4), 1131–1140. <https://doi.org/10.1007/s12517-011-0428-y> <https://doi.org/>.
- Andersen, I.M., Williamson, T.J., Gonzalez, M.J., Vanni, M.J., 2020. Nitrate, ammonium, and phosphorus drive seasonal nutrient limitation of chlorophytes, cyanobacteria, and diatoms in a hyper-eutrophic reservoir. *Limnol. Oceanogr.* 65 (5), 962–978. <https://doi.org/10.1002/lno.11363> <https://doi.org/>.
- Atique, U., An, K.G., 2020. Landscape heterogeneity impacts water chemistry, nutrient regime, organic matter and chlorophyll dynamics in agricultural reservoirs. *Ecol. Indic.* 110, 17. <https://doi.org/10.1016/j.ecolind.2019.105813> <https://doi.org/>.
- Chen, Y.Z., Zhu, J.R., 2018. Reducing eutrophication risk of a reservoir by water replacement: a case study of the Qingcaosha reservoir in the Changjiang Estuary. *Acta Oceanol. Sin.* 37 (6), 23–29. <https://doi.org/10.1007/s13131-018-1183-7> <https://doi.org/>.
- Dupas, R., Minaudo, C., Gruau, G., Ruiz, L., Gascuel-Oudou, C., 2018. Multidecadal trajectory of riverine nitrogen and phosphorus dynamics in rural catchments. *Water Resour. Res.* 54 (8), 5327–5340. <https://doi.org/10.1029/2018wr022905> <https://doi.org/>.
- Dupas, R., Tavenard, R., Fovet, O., Gilliet, N., Grimaldi, C., Gascuel-Oudou, C., 2016. Identifying seasonal patterns of phosphorus storm dynamics with dynamic time warping. *Water Resour. Res.* 51 (11), 8868–8882. <https://doi.org/10.1002/2015WR017338> <https://doi.org/>.
- Ferrier, R.C., Edwards, A.C., Hirst, D., Littlewood, I.G., Watts, C.D., Morris, R., 2001. Water quality of Scottish rivers: spatial and temporal trends. *Sci. Total Environ.* 265 (1–3), 327–342. [https://doi.org/10.1016/S0048-9697\(00\)00674-4](https://doi.org/10.1016/S0048-9697(00)00674-4) <https://doi.org/>.
- Gaget, V., Humpage, A.R., Huang, Q., Monis, P., Brookes, J.D., 2017. Benthic cyanobacteria: a source of cylindrospermopsin and microcystin in Australian drinking water reservoirs. *Water Res.* 124, 454–464. <https://doi.org/10.1016/j.watres.2017.07.073> <https://doi.org/>.
- Galloway, J.N., Dentener, F.J., Capone, D.G., Boyer, E.W., Howarth, R.W., Seitzinger, S. P., Asner, G.P., Cleveland, C.C., Green, P.A., Holland, E.A., Karl, D.M., Michaels, A. F., Porter, J.H., Townsend, A.R., Vorosmarty, C.J., 2004. Nitrogen cycles: past, present, and future. *Biogeochemistry* 70 (2), 153–226. <https://doi.org/10.1007/s10533-004-0370-0> <https://doi.org/>.
- Gonzalez, E.J., Ortaz, M., Penaherrera, C., de Infante, A., 2004. Physical and chemical features of a tropical hypertrophic reservoir permanently stratified. *Hydrobiologia* 522 (1–3), 301–310. <https://doi.org/10.1023/B:HYDR.0000029983.53568.d2> <https://doi.org/>.
- Grabb, K.C., Ding, S., Ning, X.Y., Liu, S.M., Qian, B., 2021. Characterizing the impact of three gorges dam on the Changjiang (Yangtze River): a story of nitrogen biogeochemical cycling through the lens of nitrogen stable isotopes. *Environ. Res.* 195, 110759 <https://doi.org/10.1016/j.envres.2021.110759> <https://doi.org/>.
- Guo, Z.F., Yan, C.Z., Wang, Z.S., Xu, F.F., Yang, F., 2020. Quantitative identification of nitrate sources in a coastal peri-urban watershed using hydrogeochemical indicators

- and dual isotopes together with the statistical approaches. *Chemosphere* 243, 125364. <https://doi.org/10.1016/j.chemosphere.2019.125364> <https://doi.org/>.
- Hao, Z., Gao, Y., Yang, T.T., Tian, J., 2017. Atmospheric wet deposition of nitrogen in a subtropical watershed in China: characteristics of and impacts on surface water quality. *Environ. Sci. Pollut. Res. Int.* 24 (9), 8489–8503. <https://doi.org/10.1007/s11356-017-8532-5> <https://doi.org/>.
- Harrison, J.A., Maranger, R.J., Alexander, R.B., Giblin, A.E., Jacinthe, P.-A., Mayorga, E., Seitzinger, S.P., Sobota, D.J., Wollheim, W.M., 2009. The regional and global significance of nitrogen removal in lakes and reservoirs. *Biogeochemistry* 93 (1–2), 143–157. <https://doi.org/10.1007/s10533-008-9272-x> <https://doi.org/>.
- He, G.J., Fang, H.W., Bai, S., Liu, X.B., Chen, M.H., Bai, J., 2011. Application of a three-dimensional eutrophication model for the Beijing Guanting Reservoir, China. *Ecol. Model.* 222 (8), 1491–1501. <https://doi.org/10.1016/j.ecolmodel.2010.12.006> <https://doi.org/>.
- Hecky, R.E., Kilham, P., 1988. Nutrient limitation of phytoplankton in freshwater and marine environments: a review of recent evidence on the effects of enrichment. *Limnol. Oceanogr.* 33 (4), 796–822. https://doi.org/10.4319/lo.1988.33.4.part_2.0796 <https://doi.org/>.
- Huang, J.C., Zhang, Y.J., Arhonditsis, G.B., Gao, J.F., Chen, Q.W., Peng, J., 2020. The magnitude and drivers of harmful algal blooms in China's lakes and reservoirs: a national-scale characterization. *Water Res.* 181, 115902. <https://doi.org/10.1016/j.watres.2020.115902> <https://doi.org/>.
- Huisman, J., Codd, G.A., Paerl, H.W., Ibelings, B.W., Verspagen, J.M.H., Visser, P.M., 2018. Cyanobacterial blooms. *Nat. Rev. Microbiol.* 16 (8), 471–483. <https://doi.org/10.1038/s41579-018-0040-1> <https://doi.org/>.
- Jones, J.R., Knowlton, M.F., An, K.G., 2003. Trophic state, seasonal patterns and empirical models in South Korean reservoirs. *Lake Reserv. Manag.* 19 (1), 64–78. <https://doi.org/10.1080/07438140309353991> <https://doi.org/>.
- Komatsu, E., Fukushima, T., Shiraishi, H., 2006. Modeling of P-dynamics and algal growth in a stratified reservoir—mechanisms of P-cycle in water and interaction between overlying water and sediment. *Ecol. Model.* 197 (3–4), 331–349. <https://doi.org/10.1016/j.ecolmodel.2006.03.023> <https://doi.org/>.
- Kong, X.Z., Zhan, Q., Boehrer, B., Rinke, K., 2019. High frequency data provide new insights into evaluating and modeling nitrogen retention in reservoirs. *Water Res.* 166, 115017. <https://doi.org/10.1016/j.watres.2019.115017> <https://doi.org/>.
- Leigh, C., Burford, M.A., Roberts, D.T., Udy, J.W., 2010. Predicting the vulnerability of reservoirs to poor water quality and cyanobacterial blooms. *Water Res.* 44 (15), 4487–4496. <https://doi.org/10.1016/j.watres.2010.06.016> <https://doi.org/>.
- Li, J.Z., Tan, S.M., 2015. Nonstationary flood frequency analysis for annual flood peak series, adopting climate indices and check dam index as covariates. *Water Resour. Manag.* 29 (15), 5533–5550. <https://doi.org/10.1007/s11269-015-1133-5> <https://doi.org/>.
- Li, M.J., Liu, Z.W., Zhang, M.D., Chen, Y.C., 2021. A workflow for spatio-seasonal hydrochemical analysis using multivariate statistical techniques. *Water Res.* 188, 116550. <https://doi.org/10.1016/j.watres.2020.116550> <https://doi.org/>.
- Li, X., Huang, T.L., Ma, W.X., Sun, X., Zhang, H.H., 2015. Effects of rainfall patterns on water quality in a stratified reservoir subject to eutrophication: implications for management. *Sci. Total Environ.* 521–522, 27–36. <https://doi.org/10.1016/j.scitotenv.2015.03.062> <https://doi.org/>.
- Liang, Z.Y., Soranno, P.A., Wagner, T., 2020. The role of phosphorus and nitrogen on chlorophyll a: evidence from hundreds of lakes. *Water Res.* 185, 116236. <https://doi.org/10.1016/j.watres.2020.116236> <https://doi.org/>.
- López, J., Francés, F., 2013. Non-stationary flood frequency analysis in continental Spanish rivers, using climate and reservoir indices as external covariates. *Hydrol. Earth Syst. Sci.* 17 (8), 3189–3203. <https://doi.org/10.5194/hess-17-3189-2013> <https://doi.org/>.
- Lottig, N.R., Tan, P.N., Wagner, T., Cheruvilil, K.S., Soranno, P.A., Stanley, E.H., Scott, E., Stow, C.A., Yuan, S., 2017. Macroscale patterns of synchrony identify complex relationships among spatial and temporal ecosystem drivers. *Ecosphere* 8 (12), e02024. <https://doi.org/10.1002/ecs2.2024> <https://doi.org/>.
- Mamun, M., Kwon, S., Kim, J.E., An, K.G., 2020. Evaluation of algal chlorophyll and nutrient relations and ratios along with trophic status, light regime in 60 Korea reservoirs. *Sci. Total Environ.* 741. <https://doi.org/10.1016/j.scitotenv.2020.140451> <https://doi.org/>.
- Matyas, K., Oldal, I., Korponai, J., Tatrai, I., Paulovits, G., 2003. Indirect effect of different fish communities on nutrient chlorophyll relationship in shallow hypertrophic water quality reservoirs. *Hydrobiologia* 504 (1–3), 231–239. <https://doi.org/10.1023/b:hydr.0000008523.83752.14> <https://doi.org/>.
- McMeans, B.C., McCann, K.S., Guzzo, M.M., Bartley, T.J., Bieg, C., Blanchfield, P.J., Fernandes, T., Giacomini, H.C., Middel, T., Rennie, M.D., Ridgway, M.S., Shuter, B. J., 2020. Winter in water: differential responses and the maintenance of biodiversity. *Ecol. Lett.* 23 (6), 922–938. <https://doi.org/10.1111/ele.13504> <https://doi.org/>.
- Miller, T., Svoboda, Z., Meller, E., Poleszczuk, G., 2016. Globokie Lake in Szczecin after hydrotechnical regulations. *Ecol. Chem. Eng. S* 23 (1), 71–86. <https://doi.org/10.1515/cees-2016-0005> <https://doi.org/>.
- Qi, C., Zhou, Y., Xu, X.G., Zhang, L.M., Lin, H., Wu, X.T., Shi, K., Wang, G.X., 2019. Dynamic monitoring of resuspension in the multiple eco-types of the littoral zone of a shallow wind-disturbed lake. *Aquat. Sci.* 81 (2). <https://doi.org/10.1007/s00027-019-0620-9> <https://doi.org/>.
- Qin, B.Q., Zhou, J., Elser, J.J., Gardner, W.S., Deng, J.M., Brookes, J.D., 2020. Water depth underpins the relative roles and fates of nitrogen and phosphorus in lakes. *Environ. Sci. Technol.* 54 (6), 3191–3198. <https://doi.org/10.1021/acs.est.9b05858> <https://doi.org/>.
- Rigby, R.A., Stasinopoulos, D.M., 2005. Generalized additive models for location, scale and shape. *J. R. Stat. Soc. Appl. Stat. Ser. C* 54, 507–554. <https://doi.org/10.1111/j.1467-9876.2005.00510.x> <https://doi.org/>.
- Sakoe, H., Chiba, S., 1978. Dynamic programming algorithm optimization for spoken word recognition. *IEEE Trans. Acoust. Speech Signal Process.* 26, 43–49. <https://doi.org/10.1109/TASSP.1978.1163055> <https://doi.org/>.
- Shourian, M., Moridi, A., Kaveh, M., 2016. Modeling of eutrophication and strategies for improvement of water quality in reservoirs. *Water Sci. Technol.* 74 (6), 1376–1385. <https://doi.org/10.2166/wst.2016.322> <https://doi.org/>.
- Søndergaard, M., Lauridsen, T.L., Johansson, L.S., Jeppesen, E., 2017. Nitrogen or phosphorus limitation in lakes and its impact on phytoplankton biomass and submerged macrophyte cover. *Hydrobiologia* 795 (1), 35–48. <https://doi.org/10.1007/s10750-017-3110-x> <https://doi.org/>.
- Spears, B.M., Carvalho, L., Dudley, B., May, L., 2013. Variation in chlorophyll a to total phosphorus ratio across 94 UK and Irish lakes: implications for lake management. *J. Environ. Manage.* 115, 287–294. <https://doi.org/10.1016/j.jenvman.2012.10.011> <https://doi.org/>.
- Stagge, J.H., Rosenberg, D.E., Abdallah, A.M., Akbar, H., Attallah, N.A., James, R., 2019. Assessing data availability and research reproducibility in hydrology and water resources. *Sci. Data* 6, 190030. <https://doi.org/10.1038/sdata.2019.30> <https://doi.org/>.
- Su, C.J., Chen, X.H., 2019. Assessing the effects of reservoirs on extreme flows using nonstationary flood frequency models with the modified reservoir index as a covariate. *Adv. Water Resour.* 124, 29–40. <https://doi.org/10.1016/j.advwatres.2018.12.004> <https://doi.org/>.
- Vakili, T., Amanollahi, J., 2020. Determination of optically inactive water quality variables using Landsat 8 data: a case study in Geshlagh reservoir affected by agricultural land use. *J. Clean. Prod.* 247, 119134. <https://doi.org/10.1016/j.jclepro.2019.119134> <https://doi.org/>.
- Vilmin, L., Flipo, N., Escoffier, N., Groleau, A., 2018a. Estimation of the water quality of a large urbanized river as defined by the European WFD: what is the optimal sampling frequency? *Environ. Sci. Pollut. Res.* 25 (24), 23485–23501. <https://doi.org/10.1007/s11356-016-7109-z> <https://doi.org/>.
- Vilmin, L., Mogollon, J.M., Beusen, A.H.W., Bouwman, A.F., 2018b. Forms and subannual variability of nitrogen and phosphorus loading to global river networks over the 20th century. *Glob. Planet. Change* 163, 67–85. <https://doi.org/10.1016/j.gloplacha.2018.02.007> <https://doi.org/>.
- Wang, F.S., 2020. Impact of a large sub-tropical reservoir on the cycling of nutrients in a river. *Water Res.* 186, 116363. <https://doi.org/10.1016/j.watres.2020.116363> <https://doi.org/>.
- Wang, H.B., Shi, G.M., Tian, M., Chen, Y., Qiao, B.Q., Zhang, L.Y., Yang, F.M., Zhang, L. M., Luo, Q., 2018. Wet deposition and sources of inorganic nitrogen in the Three Gorges Reservoir Region, China. *Environ. Pollut.* 233, 520–528. <https://doi.org/10.1016/j.envpol.2017.10.085> <https://doi.org/>.
- Wang, K., Wang, P.X., Zhang, R.D., Lin, Z.B., 2020. Determination of spatiotemporal characteristics of agricultural non-point source pollution of river basins using the dynamic time warping distance. *J. Hydrol.* 583, 124303. <https://doi.org/10.1016/j.jhydrol.2019.124303> <https://doi.org/>.
- Williamson, T.J., Vanni, M.J., Renwick, W.H., 2020. Spatial and temporal variability of nutrient dynamics and ecosystem metabolism in a hyper-eutrophic reservoir differ between a wet and dry year. *Ecosystems* 24, 68–88. <https://doi.org/10.1007/s10021-020-00505-8> <https://doi.org/>.
- Xu, Y.Y., Cai, Q.H., Han, X.Q., Shao, M.L., Liu, R.Q., 2010. Factors regulating trophic status in a large subtropical reservoir, China. *Environ. Monit. Assess.* 169 (1–4), 237–248. <https://doi.org/10.1007/s10661-009-1165-5> <https://doi.org/>.
- Xu, Y.Y., Cai, Q.H., Shao, M.L., Han, X.Q., 2012. Patterns of asynchrony for phytoplankton fluctuations from reservoir mainstream to a tributary bay in a giant dendritic reservoir (Three Gorges Reservoir, China). *Aquat. Sci.* 74 (2), 287–300. <https://doi.org/10.1007/s00027-011-0221-8> <https://doi.org/>.
- Yang, C.T., Nan, J., Yu, H.Y., Li, J.H., 2020. Embedded reservoir and constructed wetland for drinking water source protection: effects on nutrient removal and phytoplankton succession. *J. Environ. Sci.* 87, 260–271. <https://doi.org/10.1016/j.jes.2019.07.005> <https://doi.org/>.
- Zhang, L.Y., Tian, M., Peng, C., Fu, C., Li, T.Z., Chen, Y., Qiu, Y., Huang, Y.M., Wang, H. B., Li, Z., Yang, F.M., 2020. Nitrogen wet deposition in the Three Gorges Reservoir area: characteristics, fluxes, and contributions to the aquatic environment. *Sci. Total Environ.* 738, 140309. <https://doi.org/10.1016/j.scitotenv.2020.140309> <https://doi.org/>.